

Measurement of the Physical Properties of Blast Waves

John M. Dewey

1 Introduction to Blast Waves

A blast wave is formed in an ambient atmosphere when there is a rapid release of energy from a concentrated source. Examples of such sources are the detonation of an exothermic material such as trinitrotoluene (TNT); nuclear fission or fusion; the rupture of a pressurized container; a spark, or the rapid heating caused by a focused pulsed laser. The sudden release of energy causes the material of a symmetrical centered source to expand rapidly as a spherical piston. This piston produces a compression wave in the ambient gas. If the speed of the piston is fast enough, or of long enough duration, the compression wave develops into a shock wave. A shock wave is characterized by the very rapid increase, within a distance of about ten mean-free-path lengths, of all the physical properties of the ambient gas, namely, the hydrostatic pressure, density, particle velocity, temperature and entropy. Immediately behind the shock front the properties decay in an exponential fashion, and in the cases of hydrostatic pressure and density will fall below the values of the ambient atmosphere. The particle velocity also decreases until it comes to rest and begins to move in the opposite direction. A typical time-history of a physical property such as hydrostatic pressure, density, particle velocity and dynamic pressure at a fixed point in a blast wave is shown in Fig. 1.

The period when the physical properties are above the ambient value is known as the positive phase, and the period when the properties are below the ambient value is the negative phase. The duration of the positive phase is slightly different for each of the physical properties. Close to the minimum of the negative phase a second

J.M. Dewey (✉)

Department of Physics and Astronomy, University of Victoria, Victoria,
BC V8P 5C2, Canada
e-mail: jdewey@uvic.ca

J.M. Dewey

Dewey McMillin and Associates Ltd, Victoria, BC, Canada

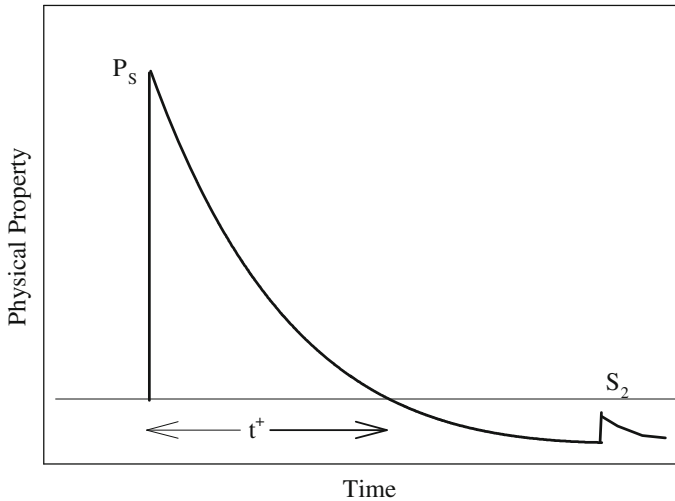


Fig. 1 The form of a time-history of hydrostatic pressure, density, particle velocity or dynamic pressure at a fixed point in a free-field blast wave. P_s is the peak value immediately behind the primary shock, S_2 the second shock, and t^+ the duration of the positive phase

shock arrives, produced by the over expansion and subsequent implosion of the detonation products or source materials.

2 The Physical Properties of Blast Waves

A uniform chemical detonation rapidly produces a high-pressure, high-temperature sphere of gas, which expands in the ambient medium to produce a spherical shock wave. The contact surface between the detonation products and the ambient gas soon becomes irregular and there is considerable mixing of the two gases (Brouillette) [1], but only in extreme cases, such as when there has been a non-symmetrical detonation, does this affect the uniformity of the expanding spherical shock. The release of energy from a detonation is rapid, but not instantaneous, and the rate of energy release has a small but measurable effect on the physical properties of the resulting blast wave. Some of the energy from an explosion may be released as radiation: about 5 % from a TNT detonation, and approximately 50 % from a nuclear explosion. If the explosion is on or close to the ground some of the energy will be disbursed as seismic waves and to excavate a crater. These are some of the reasons why blast waves from different sources and at different distances from the ground, are not identical even though the nominal energy release may be the same.

A characteristic of a shock is that it causes a change of entropy in the gas through which it is passing. As the spherical shock produced by a centred explosion

expands in three dimensions, it monotonically decays in strength and leaves the air in a state of radially decreasing entropy and temperature. This means that there are no simple thermodynamic relationships between the physical properties of the gas passing a fixed point in a blast wave. In other words, if, for example, the time-history of hydrostatic pressure is measured at a fixed point, it is not possible to calculate the time-histories of the density or temperature from that measurement. To fully describe the physical properties of a gas element in a blast wave it is necessary to independently measure at least three of the physical properties, such as, hydrostatic and total pressures, and density or particle velocity.

More detailed information about the physical properties of blast waves is provided by Needham [2] and Dewey [3].

2.1 Definitions of the Physical Properties

In order to interpret and relate the measured physical properties of a blast wave it is important to have a precise understanding of the definitions of those properties. A powerful tool in the study of blast waves is the fact that for most explosives the physical properties accurately scale for charge mass, over several orders of magnitude, and for a large range of ambient atmospheric conditions. The appropriate Hopkinson's and Sachs' scaling laws are described in Sect. 4. In order for the physical properties to be used in these scaling laws they are usually reported in terms of the values of those properties in the ambient atmosphere, e.g. P/P_0 , ρ/ρ_0 and T/T_0 , where P is the hydrostatic pressure, ρ the density, and T the absolute temperature, and the suffix 0 indicates the value in the ambient atmosphere. The strength of the shock front at the leading edge of the blast wave is usually stated in terms of its Mach number relative to the speed of sound in the ambient atmosphere, i.e. $M_S = V_S/a_0$, where M_S is the shock Mach number, V_S shock velocity, and a_0 the ambient sound speed.

2.1.1 Hydrostatic Pressure

The hydrostatic pressure of a gas is defined as the force per unit area on a surface caused by the random motion of the molecules in the gas. It does not include any component due to the translational movement of the gas, and therefore can only be measured by a transducer that is flush mounted in a surface that is parallel to the flow in a blast wave. It is a scalar quantity. In the case of a blast wave the most important feature of the hydrostatic pressure maybe that part that is greater than the ambient pressure. This is called the overpressure, viz. $OP = P - P_0$. After the passage of a blast wave the hydrostatic pressure quickly returns to the ambient value because any pressure gradients equilibrate at the rate of the local sound speed.

Hydrostatic pressure is the easiest of the physical properties of a blast wave to measure, and therefore is the property most usually quoted when defining the

magnitude or other features of the wave. Unfortunately, it is also the property that gives the least information about the blast wave because any changes of pressure dissipate at the local sound speed. An example of this is in the boundary layer which forms as the blast wave moves over the ground surface. The boundary layer in the blast wave from a large explosion is known to reach a height of about 30 cm [4]. Over that vertical distance there is no discernable change of the hydrostatic pressure, but the particle velocity, and therefore the dynamic pressure, changes from zero at the surface to what may be a very high value at the top of the boundary layer. Also, a hydrostatic pressure measurement does not detect the passage of a contact surface, such as that between the detonation products and the air, although there may be large changes in other physical properties such as density and temperature across that surface. If a hydrostatic pressure transducer does detect the passage of a contact surface, this indicates that it is also sensitive to temperature changes so that the pressure measurements may not be valid.

2.1.2 Density

The density of a gas is defined as its mass per unit volume. The time-history of density in a blast wave is similar to that for hydrostatic pressure but the initial rate of decay after the primary shock and the positive duration are not the same. The passage of a blast wave leaves the ambient atmosphere at an elevated temperature, and therefore at a density lower than that of the original ambient atmosphere. There is a residual density gradient with the lowest density at the explosion centre. The buoyancy effect of this density gradient creates the up-draught that produces the phenomenon referred to as the mushroom cloud.

2.1.3 Temperature

The temperature of a gas is defined as a measure of the kinetic energy of the random molecular motion, and its gradient indicates the direction that heat will flow. After the passage of a blast wave the gas is left in a state of radially decreasing temperature, higher than that in the original ambient atmosphere. As a result, the time-history of temperature in a blast wave is dissimilar from that shown in Fig. 1. The high temperature immediately behind the primary shock begins to decay but then starts to increase again as the warm air shocked closer to the centre of the explosion flows past the measurement location. The temperature is normally expressed in Kelvin, and as a ratio of the ambient temperature, viz. T/T_0 .

2.1.4 Particle Velocity

A feature of a blast wave, unlike a sound wave, is that there is a net translation of the gas within the wave. For scaling purposes, the particle velocity within the blast

wave is normally recorded relative to the sound speed in the ambient atmosphere, viz. u/a_0 , where u is the particle velocity and a_0 is the ambient sound speed. However, strictly speaking, this is not a Mach number because the Mach number of the flow is u/a , where a is the local speed of sound within the blast wave. The time-history of particle velocity in a blast wave is similar to that shown in Fig. 1, but the initial rate of decay and the positive duration are not the same as those for hydrostatic pressure and density. For explosives, such as TNT, that have significant after-burning of the detonation products as they mix with atmospheric oxygen, the particle velocity may have an extended positive, or outward flow, as shown by Dewey [5].

2.1.5 Dynamic Pressure

For the study of blast waves, dynamic pressure is defined as $P_D = \frac{1}{2} \rho u |u|$, where ρ is the density and u the particle velocity. Defining dynamic pressure in this way makes it into a vector rather than a scalar property. The dynamic pressure in a compressible flow is a mathematical rather than a physical property of the flow, because it is a property that cannot be directly measured. However, it can be calculated from independent simultaneous measurements of the hydrostatic and total pressures, as described in Sect. 3.8, or it can be calculated from independent measurements of the density and particle velocity. If the dynamic pressure is reported in non-dimensional units it has the form

$$\frac{P_D}{P_0} = \frac{\gamma}{2} \frac{\rho}{\rho_0} \frac{u}{a_0} \left| \frac{u}{a_0} \right| \quad (1)$$

where γ is the ratio of specific heats, which for air is 1.4, and the other parameters are as previously defined. The dynamic pressure time-history in a blast wave is similar to that shown in Fig. 1, and the positive duration will be identical to that for particle velocity.

The loading on a structure caused by the translational motion of the gas within the blast wave, sometimes called the drag loading, is usually stated as the product of the dynamic pressure and a drag coefficient. In the rapidly varying dynamic pressure of a blast wave the drag coefficient may not have a constant value, and may be a function of the local Mach number and/or the Reynolds number. This problem is discussed, relative to the loading on a cylindrical structure, by van Netten and Dewey [6]. Most of the damage caused by a blast wave to above ground structures is due to the drag loading, although the damage criteria are usually related to the peak value and the positive-duration impulse of hydrostatic pressure.

2.1.6 Reflected Pressure

When the primary shock of a blast wave strikes a plane surface that is face-on to the blast it is reflected normal to the surface, and the gas behind the shock is brought to rest non-isentropically so that the translational kinetic energy is added to the hydrostatic pressure. The resulting pressure on the surface is known as the reflected pressure. The reflected pressure is the largest loading force that can be produced by a blast wave, but its duration at a point on the reflecting surface is determined by the distance of that point from the closest edge of the structure. If the plane reflecting surface is finite in size, the reflected pressure, P_R , will be relieved by a rarefaction wave generated as the reflected shock diffracts around the boundary of the reflecting surface, as illustrated in Fig. 2. The rarefaction wave moves at the speed of sound behind the reflected shock, a_R (16). After the arrival of the head of the rarefaction wave, the pressure on the reflecting surface decreases to what is known as the total pressure.

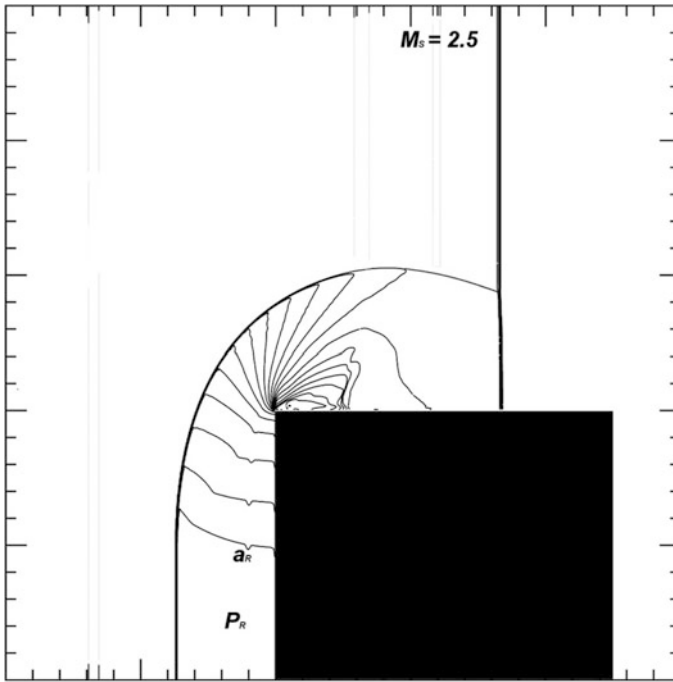


Fig. 2 Numerical simulation of a Mach 2.5 shock incident on a rigid structure. The lines shown between the reflected shock and the structure are isopycnics. (Courtesy A.A. van Netten)

2.1.7 Total Pressure

Total or stagnation pressure, P_T , is defined as the pressure exerted on a surface which is face-on to the flow, as a result of the flow being brought to rest isentropically. Work is done both to bring the gas to rest and to compress it adiabatically. After the reflected pressure has been relieved by the arrival of the rarefaction wave from the closest edge of the reflecting surface, the reflected shock moves back into the incoming flow generated by the blast wave. If the Mach number of the primary shock of the blast wave is less than 2.0681, the reflected shock will continue to move backwards against the flow, becoming increasingly weaker. If the Mach number of the primary shock of the blast wave is greater than 2.0681, the reflected shock will move back until its speed is matched by that of the incoming flow, and it will form a bow shock around the structure. In this case, the gas flow impinging on the surface and causing the total pressure will have passed through the bow shock, which will change the physical properties of the gas. As result, the relationship of the total pressure to the physical properties of the blast wave depends on whether the Mach number of the primary shock is greater or less than 2.0681 [see (13) & (14)].

2.1.8 Loading Pressure

The loading pressure is the pressure on any surface of a structure exposed to a blast wave. It can be measured by a pressure transducer flush mounted in the surface and is strongly influenced by the orientation of the surface, and the shape and size of the structure.

3 Measurement Techniques

The sections below describe many of the methods that have been used to measure the physical properties of blast waves. Reisler et al. [7] provides, in three volumes, a complete compendium of all the blast wave measurement techniques and instrumentation used by the United States and several of its NATO allies between 1943 and 1993. The previous reference does not contain information about photogrammetric methods applied to the measurement of blast waves, and these techniques are described in Dewey [8–10].

3.1 Primary-Shock Velocity Analysis

One of the easiest measurement techniques to implement, and which gives accurate values of the physical properties immediately behind the primary shock, is an analysis of the primary shock velocity using the Rankine-Hugoniot equations [11].

There are several ways by which the times-of-arrival of the primary shock can be measured at a series of positions at known distances from the charge centre. The pressure transducers described in Sect. 3.2 can provide this information. Alternatively, a series of simple time-of-arrival detectors connected by a single cable to a recording device can be used as described by Dewey [12]. The highest density of time-of-arrival data can be obtained from high-speed photography of the refractive image of the expanding blast as described in Sect. 3.9.1. In order to use these radius-time data to calculate the physical properties immediately behind the shock it is necessary to calculate the shock velocity. The average velocity between two relatively close detectors can be calculated by dividing the distance between the detectors by the difference between the two times of arrival. When a continuous series of time-of-arrival data is available, the shock velocity at any position can be determined by differentiation of an equation fitted by least squares to the radius-time data.

The primary-shock velocity decays monotonically with radius, from a Mach number of about three as it emerges from the detonation products, until it asymptotically approaches the ambient speed of sound at larger radii. It is important that any equation used to describe the radius-time measurements reflect this monotonic decay. For this reason, a polynomial equation is not suitable because it will have a non-monotonically decaying slope. Dewey [13] proposed the following equation for this purpose, and it has been used successfully since that time to describe the radius-time trajectories of the primary shocks of the blast waves from a variety of centred explosive sources:

$$R_s = A + a_0 t_s + C \ln(1 + a_0 t_s) + D \sqrt{\ln(1 + a_0 t_s)}, \quad (2)$$

where R_s is the shock radius, t_s the time-of-arrival of the shock at that radius, a_0 the speed of sound in the ambient air and A , C and D are the least-squares fitted coefficients.

If it is applied over a wide range of distances, the relative error of measuring R_s and t_s at larger radii may be greater than the error for measurements closer to the charge. In this case, the goodness of the least squares fit may be better at large rather than small radii. This problem can be overcome by weighting the data by $1/R_s^2$ to emphasise the fit at small radii, and by $1/R_s$ at intermediate distances. The implementation of this technique is illustrated in Kleine et al. [14].

The time derivative of Eq. (2) is

$$\frac{dR_s}{dt_s} = a_0 \left(1 + \frac{C}{1 + a_0 t_s} + \frac{D}{2(1 + a_0 t_s) \sqrt{\ln(1 + a_0 t_s)}} \right) \quad (3)$$

so that as $t_s \rightarrow \infty$, the speed of the shock approaches the ambient sound speed, and the Mach number of the shock, M_s , at any other time is given by

$$M_s = \frac{1}{a_0} \frac{dR_s}{dt_s} \quad (4)$$

This value of the shock Mach number can be used in the Rankine-Hugoniot equations to determine the values of all the physical properties immediately behind the shock, as follows, where the ambient atmosphere is assumed to be air with a ratio of specific heats $\gamma = 1.4$, and the properties are given as ratios of the ambient values. The suffices $_s$ and $_0$ respectively indicate the value immediately behind the shock and the ambient value.

Hydrostatic pressure:

$$\frac{P_s}{P_0} = \frac{7M_s^2 - 1}{6}; \quad (5)$$

hydrostatic overpressure:

$$\frac{OP_s}{P_0} = \frac{7(M_s^2 - 1)}{6}; \quad (6)$$

density:

$$\frac{\rho_s}{\rho_0} = \frac{6M_s^2}{M_s^2 + 5}; \quad (7)$$

particle velocity:

$$\frac{u_s}{a_0} = \frac{5}{6} \left(\frac{M_s^2 - 1}{M_s} \right); \quad (8)$$

absolute temperature:

$$\frac{T_s}{T_0} = \frac{(7M_s^2 - 1)(M_s^2 + 5)}{36M_s^2}; \quad (9)$$

sound speed:

$$\frac{a_s}{a_0} = \frac{1}{6M_s} \sqrt{(7M_s^2 - 1)(M_s^2 + 5)}; \quad (10)$$

local sound speed:

$$\frac{u_s}{a_s} = \frac{5(M_s^2 - 1)}{\sqrt{(7M_s^2 - 1)(M_s^2 + 5)}}; \quad (11)$$

dynamic pressure:

$$\frac{P_{Ds}}{P_0} = \frac{35}{12} \frac{(M_s^2 - 1)^2}{(M_s^2 + 5)}; \quad (12)$$

total overpressure (subsonic case, $M_s < 2.0681$):

$$\frac{OP_{Ts}}{P_0} = \frac{7M_s^2 - 1}{6} \left[\frac{12M_s^2(M_s^2 + 2)}{(M_s^2 + 5)(7M_s^2 - 1)} \right]^{3.5} - 1; \quad (13)$$

total overpressure (supersonic case, $M_s > 2.0681$):

$$\frac{OP_{Ts}}{P_0} = \frac{67920.1(M_s^2 - 1)^7}{(M_s^2 + 5)(42M_s^4 - 96M_s^2 + 45)^{2.5}} - 1; \quad (14)$$

reflected overpressure:

$$\frac{OP_{Rs}}{P_0} = \frac{(7M_s^2 - 1)(4M_s^2 - 1)}{3(M_s^2 + 5)} - 1; \quad (15)$$

reflected sound speed, a_r : (a_r is the sound speed behind the reflected shock and therefore the speed at which the rarefaction wave from the edge of a structure will move across the surface, reducing the reflected pressure¹)

$$\frac{a_R}{a_0} = \frac{\sqrt{(M_s^2 + 2)(4M_s^2 - 1)}}{3M_s}; \quad (16)$$

increase of entropy, ΔS , of the gas passing through the shock:

$$\Delta S = 8.3143 \ln \left[\frac{(7M_s^2 - 1)^{2.5}}{46656} \left(\frac{M_s^2 + 5}{M_s^2} \right)^{3.5} \right] \text{ J mole}^{-1} \text{ K}^{-1}. \quad (17)$$

The above Rankin-Hugoniot relationships are derived from the two possible states of a compressible fluid for which the mass, momentum and energy are conserved, and provide values of the physical properties of the gas immediately behind the shock that are completely reliable, such that they are the preferred method of calibrating electronic transducers, such as those discussed below. For strong shocks with a Mach number greater than about 3.5, corresponding to a peak

¹Knowing a_R and the distance from a point on a normally reflecting surface to the nearest edge of the surface, permits a calculation of the duration of the reflected pressure at that point before it is relieved by the arrival of the rarefaction wave from the edge of the surface.

hydrostatic overpressure greater than 13 atm, additional degrees of freedom of the gas are excited and for exact results it is necessary to use a real-gas equation of state to correct the above relationships.

3.2 *Hydrostatic Pressure Gauges*

Hydrostatic pressure is the easiest physical property to measure directly in a blast wave, and is therefore the one most widely used. A pressure transducer is normally a metal diaphragm that is displaced by the loading of the blast wave, and the amount of displacement is sensed by a piezo-electric crystal, a capacitor or a strain transducer. The signals from the transducer may be pre-amplified by a device close to the gauge before being transmitted by cable to an amplifier and storage device. A piezoelectric transducer produces a change of voltage but is unable to generate a significant current, and so the pre-amplifier for such a device needs to be a charge amplifier. A pressure gauge used to monitor a blast wave may be exposed to thermal radiation from the explosion, and heated by the blast wave itself. It is important therefore that it be insensitive to these thermal effects, and this can be tested by exposing the gauge to a thermal source, such as an infrared lamp, and ensuring that no signal is generated by this exposure. Also, the gauge must be isolated from the structure in which it is mounted so that stresses in the mount do not strain the case of the gauge and generate spurious signals.

To measure the hydrostatic pressure the transducer must be mounted so that the surface of the diaphragm is parallel to the flow within the blast wave. For a hemispherical surface-burst explosion, or in the Mach reflection region of an airburst explosion, this can be done by flush mounting the gauge in the ground surface. The gauge will be in the boundary layer, but there is no change in hydrostatic pressure through a boundary layer. To measure the hydrostatic pressure in the blast wave from a spherical airburst explosion the gauge must be mounted in a disc-shaped baffle with a sharp-edged rim, sometimes called a lollipop or pancake mount, or in the side of a sharp pointed cylinder. To minimise edge effects, experience has shown that the radius of the disc, or the distance of the cylinder mounted gauge from the pointed tip, should be at least 10 times the thickness of the disc or the diameter of the cylinder. In both cases the bevel length should be at least seven times the thickness or diameter. The disc or cylinder must be mounted on a long arm to minimise the effects of shocks, compression and rarefaction waves reflected from the stand holding the gauge. These waves will travel back towards the transducer against the blast wave flow at a speed of $a - u$, where a is the local sound speed and u the particle velocity within the blast wave. This type of baffle must be carefully aligned with the centre of the charge because any misalignment will cause the primary shock to strike the transducer at an angle, thus not measuring the hydrostatic pressure, and will generate additional noise due to the non-symmetry of the blast as it passes the trailing edge of the baffle. An array of gauge-mounts such as those described above, deployed on a large scale test, is shown in Fig. 3.

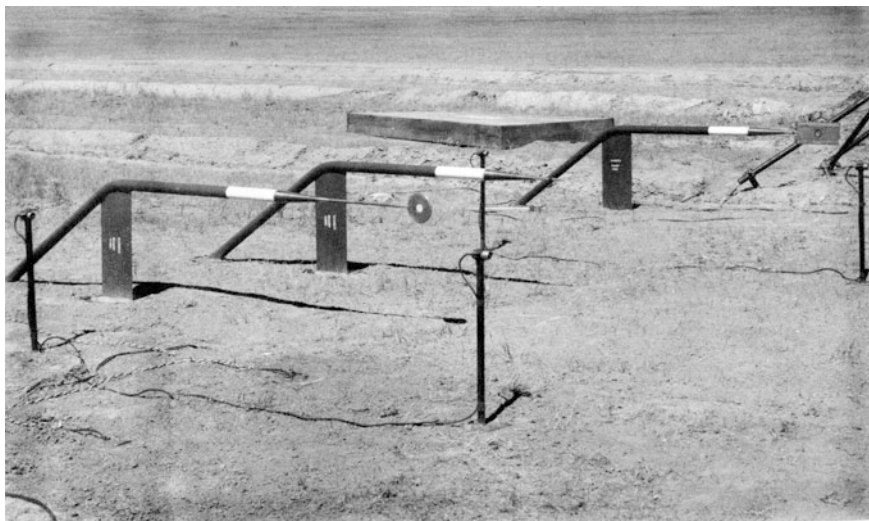


Fig. 3 An array of pressure gauges deployed on a large scale test. From lower left to right: a pair of face-on time-of-arrival detectors to measure the shock velocity; a lollipop or pancake mount; a cylindrical mount; another pair of time-of-arrival detectors, and a rectangular baffle [7]

Pressure transducers supplied by a manufacturer will normally be accompanied by a calibration curve relating the imposed pressure to the output voltage. Ideally, this relationship should be as linear as possible. The calibration may change with time, and particularly with use, and so the gauge should be regularly recalibrated, ideally before and after each exposure to a blast wave, and with the pre-amplifier, amplifier and recorder used for the exposure. With some calibration systems a measured pressure is applied to the transducer and then rapidly released. However, this monitors an outward deflection of the diaphragm rather than an inward deflection as would be caused by the passage of a blast wave. A preferred method of calibration is to use a simple shock tube, with the transducer flush mounted in the wall of the tube, and with a sensor on each side of the transducer to measure the shock velocity, from which the shock Mach number can be calculated. This Mach number is then used in (5) or (6) to determine the change of pressure as the shock moved across the transducer. Pressure gauges can be calibrated in situ on a test site using a portable, flexible, valve driven shock tube with the open end of the tube being held firmly over the transducer. The Mach number of the calibrating shock can be measured using a pair of sensors installed close to the end of the tube, and the reflected pressure to which the transducer is subjected can be calculated using (15).

Some companies that supply pressure transducers and auxiliary equipment for the measurement of blast and shock waves are: PCB (www.pcb.com), Endevco (www.endevco.com) and Kistler (www.kistler.com).

The recorded signal from a pressure transducer is converted to a pressure-time history by application of the pressure-voltage calibration relationship. The changing

pressure at the shock front is virtually instantaneous because the thickness of the shock is estimated to be about 10 mean-free-path lengths. In order to measure this very rapid pressure change the transducer needs to have a high frequency response, but this may result in signal over-shoot and ringing. To overcome this affect the manufacturer may introduce mechanical and/or electronic damping of the signal, but if too much damping is applied the peak signal may be rounded and not record the maximum value. The manufacturer must make a compromise between these two effects, but in any event the estimation of peak pressure from a pressure-time history needs careful interpretation.

The decay of pressure behind the primary shock usually has an exponential form, in which case the peak can be estimated by least squares fitting a section of the pressure-time data to an exponential decay, viz.

$$P = P_s e^{-\alpha t}, \quad (18)$$

where P and t are respectively the measured values of pressure and time measured from the time of arrival of the primary shock, in the region close to the shock, and P_s and α are the least-squares fitted coefficients. P_s is a good estimate of the peak pressure immediately behind the shock. If the pressure-time history from the primary shock to the second shock has the classic form similar to that shown in Fig. 1, the measured overpressure data may be well described by a least squares fit to the modified Friedlander equation, viz.

$$OP = OP_s e^{-\alpha t} \left(1 - \frac{t}{t^+}\right), \quad (19)$$

where P_s , α and t^+ are the fitted coefficients to the measured P , t data. Usually, P_s and t^+ are good estimates of the peak pressure and the positive duration, respectively. Equation (19) can be integrated between $0 < t < t^+$ to give the overpressure impulse in the positive phase, viz.

$$I = \int_0^{t^+} OP_s e^{-\alpha t} \left(1 - \frac{t}{t^+}\right) dt = OP_s \frac{1}{\alpha^2 t^+} \left(e^{-\alpha t^+} - 1 + \alpha t^+\right) \quad (20)$$

3.3 Total (Stagnation) Pressure

Total pressure, as defined in Sect. 2.1.7, can be measured by the same type of electronic transducer as used to measure hydrostatic pressure, but with the surface face-on to the blast. There should be no flow across the surface of the transducer, which is held in a pencil or cylindrical mount, and is slightly recessed by a few millimetres to eliminate any trans-surface flow. The gauge must be supported on a narrow arm in order to minimise the effect of waves reflecting from the main

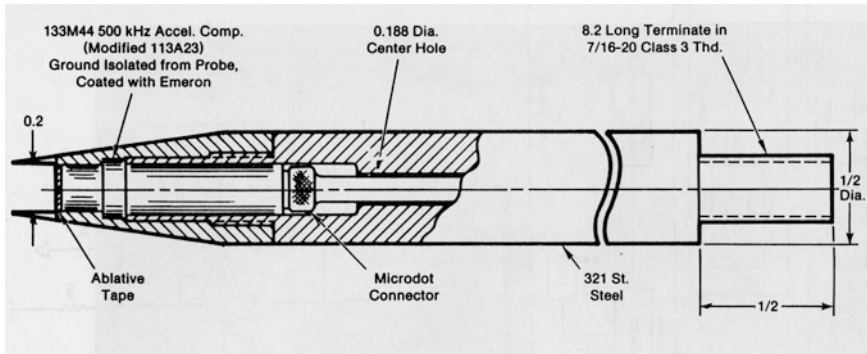


Fig. 4 A drawing of the design of a total-pressure gauge [7]. The units of the dimensions shown are inches. The front surface of the pressure transducer is set back 0.2 in. from the tip of the probe

support. It is important that the gauge be pointed directly at the charge centre to eliminate any transverse flow across the surface of the transducer. A pressure transducer can also be flush mounted in the side of the cylinder holding the total-pressure transducer to obtain a simultaneous measurement of the hydrostatic pressure. A diagram of the design of a total-pressure gauge is shown in Fig. 4.

The total-pressure transducer will initially record the reflected pressure (Sect. 2.1.6), but this will be relieved in the few micro-seconds that it takes for the rarefaction wave, created by the diffraction of the reflected shock around the edge of the mount holding the transducer, to reach the surface of the transducer. This short duration reflected-pressure measurement will appear as a spike at the beginning of the total-pressure measurement, but because of its very short duration may not be a reliable measure of the reflected pressure.

3.4 Loading Pressure

The loading pressure time-history at any point on the surface of a structure exposed to a blast wave can be measured by a pressure transducer flush mounted in the surface at that point.

3.5 Density

The density of the gas within a blast wave has been measured by devices that monitor the soft β radiation from radioactive sources such as erbium, ^{169}Er , and promethium, ^{147}Pm , (Dewey & Anson [15]; Ritzel [16]). The radioactive source in such a device is mounted in a sharp edged baffle a few centimetres from the

radiation detector which is mounted in a similar baffle. The density gauge can be calibrated by passing aluminium and plastic foils of known aerial density between the source and the detector. The baffles holding the source and the detector in the gauge described by Dewey and Anson [15] had sharp leading edges but rectangular trailing edges. As a result, the shocks and rarefaction waves generated by the primary shock as it diffracted around the blunt ends of the baffles travelled back between the baffles against the blast wave flow and disturbed the measurement of the density-time history. This error was corrected in future versions of the density gauge by using baffles with sharp leading and trailing edges [16].

The density gauge described by Slater et al. [17] was incorporated in a blast gauge station that, in addition to measuring the density-time history, also measured the hydrostatic and total pressures, and the speed of the shock as it traversed the gauge (Fig. 5).

3.6 *Temperature*

There appear to have been no successful techniques to accurately and directly measure the temperature of the air in a blast wave. A temperature transducer, such as a thermistor or a resistor, must be supported on a substrate that will have a high thermal capacity and the transducer measures the temperature of that substrate rather than the air in the blast wave. In addition, it is difficult to shield a temperature transducer from the thermal radiation of the detonating charge without affecting the properties of the blast wave passing over the transducer. The temperature is calculated, therefore, from the other physical properties that can be more easily measured, viz.

$$\frac{T}{T_0} = \frac{P}{P_0} \frac{\rho_0}{\rho}, \quad (21)$$

where T is the absolute temperature, P the hydrostatic pressure, ρ the density and the suffix 0 indicates the values in the ambient atmosphere.

3.7 *Particle Velocity*

The particle velocity throughout a blast wave flow field has been measured using high-speed photography of an array of flow tracers established immediately before the detonation of the charge [5]. The technique for doing this is described in more detail in Sect. 3.9.2. The time-history of particle velocity in free-field blast waves from centred charges of explosives such as nitro-glycerine, Pentolite, C4 and ammonium-nitrate fuel-oil (ANFO) is well described by the modified Friedlander

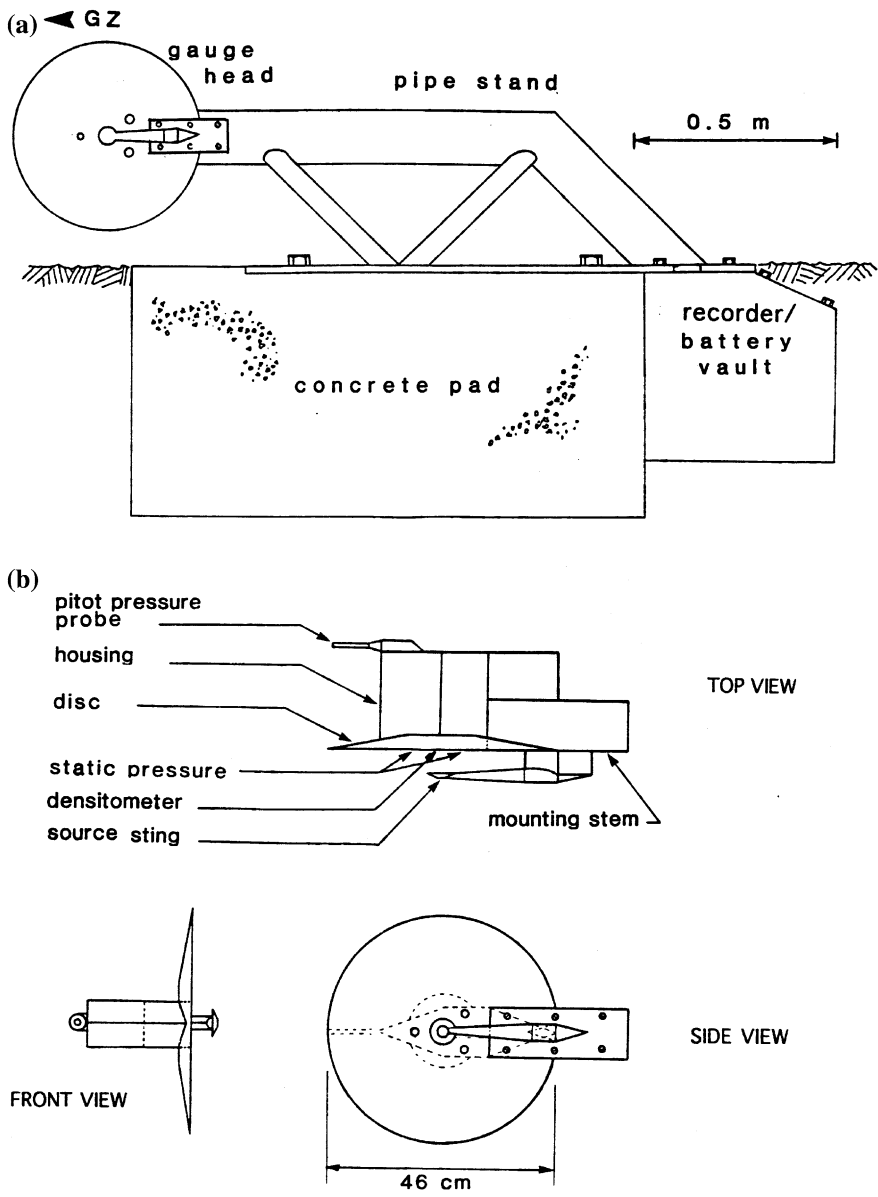


Fig. 5 Diagram of Suffield Blast Station [17] to make simultaneous, independent measurements of hydrostatic and total pressures, density and shock velocity

equation (19), but due to the after-burning of TNT, Dewey [5] suggested that the time history of particle velocity for that explosive was better described by

$$u = u_s e^{-\alpha t} (1 - \beta t) + A \ln(1 + \beta t) \quad (22)$$

where u is the particle velocity at time t after the arrival of the primary shock, u_s is the peak particle velocity immediately behind the shock, and α , β and A are least-squares fitted coefficients.

3.8 Dynamic Pressure

The dynamic pressure in a compressible fluid, as defined in 2.1.5, is a mathematical rather than a physical property of the flow in that it cannot be directly measured by a transducer inserted into the flow. The dynamic pressure in a blast wave can be calculated by inserting the independently measured particle velocity, u , and density, ρ , into (1), or from independent and simultaneous measurements of the total and hydrostatic pressures, P_T and P , respectively.

The functional relationship to calculate the dynamic pressure from the total and hydrostatic pressures depends on whether the flow is locally sub-or super-sonic, that is, whether $M_u \leq 1$ or > 1 , where $M_u = u/a$, u is the particle flow speed, and a the local sound speed. Since $a^2 = \gamma P/\rho$,

$$M_u^2 = \frac{\rho u^2}{\gamma P} = \frac{2P_D}{\gamma P} \quad (23)$$

and therefore

$$P_D = \frac{\gamma}{2} P M_u^2 \quad (24)$$

where P_D is the dynamic pressure and γ the ratio of specific heats. For $\gamma = 1.4$ and $M_u \leq 1$

$$P_T = P(0.2M_u^2 + 1) \quad (25)$$

which gives

$$M_u^2 = 5 \left[\left(\frac{P_T}{P} \right)^{0.286} - 1 \right] \quad (26)$$

and this value of M_u^2 can be inserted in (24) to give the dynamic pressure.

For $\gamma = 1.4$ and $M_u > 1$,

$$P_T = \frac{PM_u^2(3.58 \times 10^{-2})}{\left[1.167 - \left(\frac{0.167}{M_u}\right)\right]^{2.5}} \quad (27)$$

There is no simple algebraic solution of (27) to give M_u^2 in terms of P_T and P , and the equation must be solved iteratively or graphically to give values of M_u^2 that can be inserted in (24). Equation (27) is called the Rayleigh supersonic pitot formula. Equations (26) and (27) are derived in Liepmann and Roshko [18].

If the blast wave under study has the classical form shown in Fig. 1, the time-histories of density and particle velocity may be well described by the modified Friedlander equation (19). However, experience has shown, that the time-history of dynamic pressure is not precisely described by the modified Friedlander equation. This is to be expected because the product of two or more Friedlander equations does not have the algebraic form of the Friedlander equation, and this may lead to small errors if it is used to determine the peak dynamic pressure, the positive duration and impulse, as described in Sect. 3.2 for hydrostatic pressure. An equation of the form

$$P_D = A + Be^{-Ct} + Dt \quad (28)$$

where A , B , C and D are the least-squares fitted coefficients to the measured values of dynamic pressure, P_D , and time, t , may better describe the dynamic pressure time history than the modified Friedlander equation. (28) can be integrated to obtain the dynamic pressure impulse in the positive phase, viz.

$$I_{PD} = \int_0^{t^+} (A + Be^{-Ct} + Dt) dt = At^+ - \frac{B}{C}e^{-Ct^+} + \frac{D}{2}t^{+2} + \frac{B}{C} \quad (29)$$

where t^+ is the dynamic pressure positive phase duration. Equations (28) and (29) have been successfully used to determine the peak values, positive durations and impulses of dynamic pressure for a blast wave created by a propane/oxygen explosion [19], but to date, have not been evaluated for other explosive sources.

Setting $t = 0$ in (28) gives $P_{DS} = A + B$, where P_{DS} is the peak dynamic pressure immediately behind the primary shock. Setting $P_D = 0$ in (28) gives

$$Be^{-Ct^+} + Dt^+ = -A \quad (30)$$

where t^+ is the positive phase duration of dynamic pressure. There is no simple algebraic solution of (30) to give t^+ as a function of the other parameters, and (30) must be solved iteratively or graphically. The positive phase duration of dynamic pressure must equal that for particle velocity because of the way in which dynamic pressure is defined.

3.9 Flow Visualization Techniques

High-speed photographic techniques have been used extensively to measure the physical properties of blast waves from explosive sources ranging in size from megaton nuclear weapons to as small as 0.5 mg. These techniques have been described in general terms by Dewey [3, 8–10]. The two methods used most extensively have been a modification of shadow photography, known as refractive image analysis (RIA), and flow visualisation of particle tracers, known as particle trajectory analysis (PTA). The RIA and PTA techniques are illustrated in Fig. 6.

3.9.1 Refractive Image Analysis

The sudden increase of density at the primary shock of a blast wave causes an intense gradient of the refractive index of the ambient air, so that light passing through the shock is sharply refracted producing a distortion of the observed background, as shown in Fig. 6. This distortion can be photographed with a high-speed camera to produce a series of images from which the radius of a spherical shock can be measured as a function of time. On the lower left in Fig. 6 is an array of striped backdrops to enhance the refractive image of the shock close to the ground. The larger backdrops are 15 m high. Fiducial markers are also shown in the lower left.

The required framing rate of the camera depends on the size of the explosion. In the case of a nuclear explosion 100 frames per second is adequate [20]. For explosions in the range of 1 kt, a framing rate of about 1000 is required [21, 22], and for micro-scale charges a framing rate of the order of 1 million is needed [14].

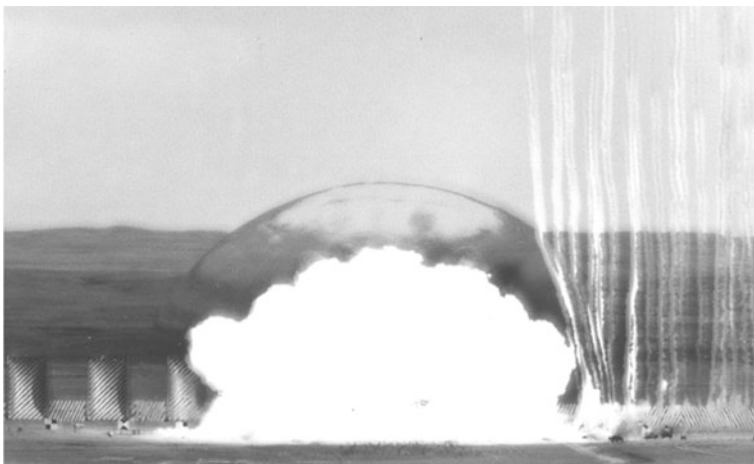


Fig. 6 A 200 t hemispherical surface-burst explosion showing the refractive image of the shock front and an array of particle-flow smoke tracers

High-speed film cameras do not run at a constant speed because of the inertia of the film spools as they are brought up to speed and then decelerated. Such cameras will normally incorporate a constant-rate timing light that will leave an image on the edge of the film. Some may leave a coded image that is related to Universal Time. The timing light is normally not immediately adjacent to the film frame that is being exposed so that there will be a displacement on the film between the exposed frame and the appropriate timing mark. This displacement must be known in order to relate the exposed frame to the correct timing mark. Digital cameras can be expected to run at the set framing rate, but this should be calibrated from time to time. Digital cameras do not provide an image with the spatial resolution of film cameras and must be used with a smaller field of view to match the resolution of film cameras.

The natural background may contain enough contrast to visualise the refractive image of the primary shock, but when very precise measurements are required, such as the accurate visualisation of the triple point region of a Mach reflection, an artificial background can be created. Such a background usually consists of a series of black and white stripes painted on boards or large canvas sails which are mounted behind the charge at a sufficient distance that they will not be struck by the blast wave until the complete blast wave in the object plane has been recorded. The precision added with such a background usually enables the second shock to also be visualised, and in rare cases the third shock. On many US and British nuclear tests such backgrounds were created to high altitudes using rockets to produce arrays of white smoke trails [20].

The refractive image of a spherical shock is recorded in the film plane of the camera that is parallel to an object plane containing the charge centre. As a result, the radius of the image measured in the film plane, r' , is not directly related to the radius of the shock, R , but to a distance, R' , in the object plane, as shown in Fig. 7 and related in (31).

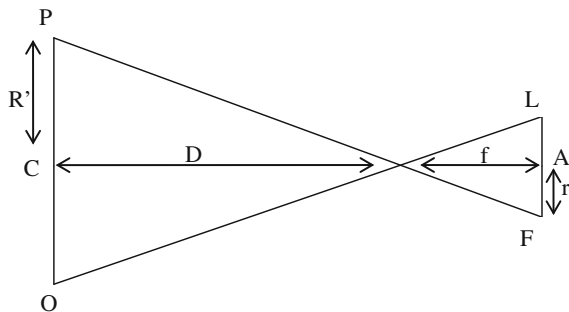


Fig. 7 Relationship between the object and film planes of a camera. CA is the central axis of the camera; OP is the object plane containing the charge centre, which is parallel to the film plane, FL ; D the distance of the centre of the object plane to the camera; f the focal length of the camera; r' a distance measured in the film plane, and R' the corresponding distance in the object plane

$$R' = \frac{r'D}{f} \quad (31)$$

where R' and r' are defined above, D is the distance of the camera lens from the charge centre and f is the focal length of the camera. The radius of the shock is then given by

$$R = D \sin \left[\tan^{-1} \frac{\cos \theta}{\left(\frac{D}{R'} - \sin \theta \right)} \right] \quad (32)$$

where θ is the offset angle of the optical axis of the camera from the charge centre, as shown in Fig. 8. This simple relationship is for the special case when the shock centre, the centre of the image plane, the shock image, and the camera are coplanar. In other situations, such as measuring the displacement of the Mach stem shock produced by an air-burst explosion, more complex three-dimensional geometric corrections must be used.

In Fig. 8, O is the centre of the spherical or hemispherical shock, S; C the camera lens; OC = D, the distance between the shock centre and the camera; CA the central axis of the camera, which is perpendicular to OP the object plane through the centre of the explosion parallel to the image plane of the camera; $\angle ACO = \theta$; $\angle QCA = \angle QOT = \alpha$; OT = R the shock radius, and OQ = R' the projection of R on the object plane. As the spherical shock expands the locus of T is a hemi-circle with diameter OC.

In order to ensure the accuracy of the measurements of the shock radius, a series of fiducial markers should be deployed in the field-of-view of the camera. Ideally, the markers should be placed in the object plane of the camera containing the charge centre, but this would significantly interfere with the blast wave flow. The fiducial markers must therefore be placed in planes beyond the charge and between the charge and the camera. The markers must be accurately survey relative to the

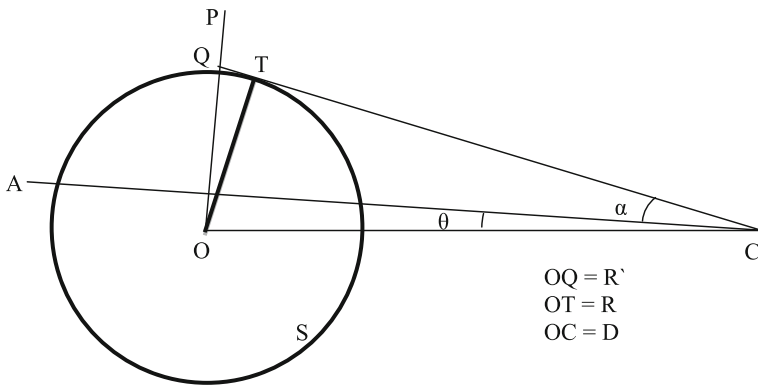
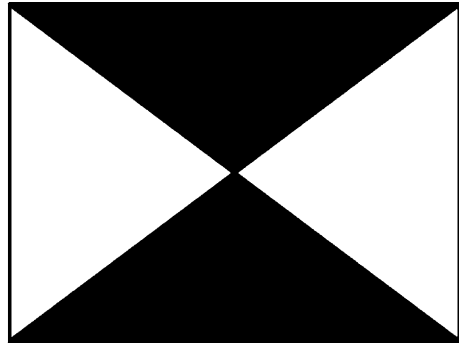


Fig. 8 Projection of the shock radius on the object plane

Fig. 9 Suggested design of a fiducial marker used to provide a length scale in the photogrammetry of the refractive image and flow tracers of blast waves



charge centre and the camera so that their positions can be geometrically projected on to the object plane. This permits confirmation of the scale used to convert the displacements measured in the film plane, r' , to the displacements in the object plane, R' , without relying entirely on (31). The design of a fiducial marker that has been found to be most effective is that shown in Fig. 9.

The survey of the fiducial markers may contain errors, and this will become apparent when the positions of the markers are projected onto the object plane and used to calculate the image scaling factor. If a single marker appears to be at fault it can be ignored. If the survey errors appear to be random, the surveyed distance of the camera from the centre of the explosion and the orientation angle of the camera can be adjusted to minimise the apparent errors in the fiducial marker positions. It is useful in the image analysis process to have fiducial markers close to the camera, which will appear in the lower left and lower right corners of the image, because these will not be concealed by dust or detonation products, and thus provide correct orientation of the image at later times in the recording.

The primary shock radius-time data obtained from high-speed photography can be used with the techniques described in Sect. 3.1 to determine the shock Mach number as a function of radius, and thus the values of all the physical properties immediately behind the shock using (5)–(17). Examples of the application of this technique are given in Kleine et al. [14] and Dewey [12].

3.9.2 Particle Trajectory Analysis

The photogrammetric technique described in Sect. 3.9.1 provides information only about the physical properties immediately behind the primary shock. In order to determine the physical properties throughout a blast wave in the radius-time plane, photogrammetric methods have been developed using the high-speed photography of flow tracers initiated a short time before charge detonation. An array of such tracers is illustrated in Fig. 6.

In order to follow accurately the flow of the air in a blast wave, particularly as it passes through the shock, a very fine particulate smoke must be used. In early

studies, such as US and British nuclear tests, a chloro-sulphuric acid mixture was used, released in a trail from a rocket or mortar shell, as described by Dewey [5]. This mixture is toxic and highly corrosive, and therefore difficult to use. In air, the mixture forms small droplets of sulphuric acid which vaporise at high temperatures so that the trail disappears for a short time behind very strong shocks. In more recent studies, smoke trails and puffs have been generated using carbon-black to produce black trails and fumed silica to produce white trails. These powders have sub-micron size particles, which remain suspended in air by the Brownian movement and have proved to be excellent tracers of the flows within blast waves, in that their velocities immediately behind a shock agree exactly with the Rankine-Hugoniot values. The smoke tracers close to the charge need to be generated a short time, e.g. 0.5 s., before the charge is detonated, and shortly before the arrival of the primary shock for tracers at greater distances. The exact time depends on the size of the explosion. The colour of the smoke that is used depends on the background against which it will be photographed. Frequently, alternate black and white tracers have been used to allow for variability of the background.

The smoke tracers should be generated in the object plane of the camera that contains the charge centre. This provides a simple relationship between measurements in the film plane of the camera and displacements of the tracers in the object plane. If the tracers are not in the object plane, a more complex geometrical manipulation is required to determine their displacements. In any event, the plane containing the smoke tracers and the charge centre must be known accurately. Accurately surveyed fiducial markers must be deployed throughout the field of view, as described in Sect. 3.9.1.

The flow tracers are observed within the varying density field of a spherical blast wave and this will deflect the optical path from a flow tracer to the camera. However, this deflection appears to be very small and not to have a significant effect on the displacement of the tracer measured from the photographic record.

Measurement of the flow-tracer trajectories in blast waves was first used only to measure the particle velocities in the radius-time plane [5]. Subsequent analyses showed that by measuring the relative distance between two adjacent flow tracers the density field could also be measured. Measuring the density at a fixed point in a blast wave does not permit calculation of the hydrostatic pressure because of the varying entropy of the gas passing that point. However, when flow tracers are used, the density is measured along the particle trajectories which are loci of constant entropy between the primary and secondary shocks. As a result, the simple adiabatic relationship between the density and pressure can be used in the Lagrangian coordinate system. Assuming that both the density and pressure immediately behind the shock, ρ_S and P_S , are known from a measurement of the shock velocity, the pressure, P , can be determined from the measured density, ρ , from

$$\frac{P}{P_S} = \left(\frac{\rho}{\rho_S} \right)^\gamma \quad (33)$$

where γ is the ratio of specific heats, and the subscript s indicates the values immediately behind the primary shock. These procedures map the hydrostatic pressure, density and particle velocity throughout the flow field in the radius-time plane, and these three properties can be used in the thermodynamic relationships to calculate all the other physical properties such as temperature, local sound speed and dynamic pressure (Dewey)[13].

Subsequently, it has been found that the measurement of the particle trajectories in a blast wave can be used more easily to map all the physical properties by using the measurements in conjunction with a hydro-code, as described in Sect. 3.11.

3.9.3 Background Oriented Schlieren

A new technique has been developed for measurement of the density field in a compressible flow, called background oriented schlieren (BOS) [23, 24]). This technique uses a digital still camera, a structured background, and inverse tomographic algorithms which can extract two-dimensional slices from a three-dimensional flow. This has been applied to obtain the density field for an axisymmetric supersonic flow over a cone-cylinder model. At this time it has not been conclusively demonstrated that the technique can be used to measure the density profile along a radial of a spherically-symmetric centred blast wave, or along any radial of an axially symmetric blast wave such as a muzzle blast, but this may be achieved in the future.

3.10 Passive Methods

Passive techniques for the measurement of the physical properties of blast waves involve the use of simple non-electronic devices that are permanently deformed or displaced by the passage of the blast wave such that the deformation or displacement can be used to estimate some property of the wave. The concept of such devices arose from the observations of the effects of explosions for which there was no, or very limited access to direct measurements. For example, when Lord Penny toured the scenes of the Hiroshima and Nagasaki nuclear events he noted that metal posts were bent by the blast waves in a uniform fashion, and that the displacement of standard Japanese gravestones was related to their distance from ground zero. On early nuclear tests, limited electronic measurements were available and some blast properties could be inferred from the degree of crushing of beer and jerry cans that had been left on the test sites. Such methods are still be used in the evaluation of accidental explosions when no direct measurements are available. As a minimum, observation of the degree of damage to simple structures can be used to estimate the relative energy release of an explosion. Details of the various passive gauges used during the US nuclear testing program are given in Reisler et al. [7].

3.10.1 Cantilever Gauges

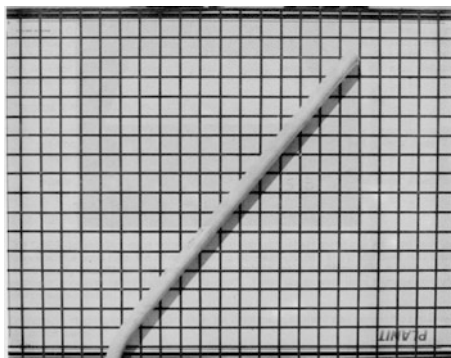
The passive device that has been used and studied most extensively is the cantilever gauge. This was based originally on the observations of the bending of metal posts by Penny [25] which he used to estimate the explosive yields of the Hiroshima and Nagasaki nuclear explosions. Early devices by Ewing and Hanna [26] and Baker et al. [27] used cantilevers with rectangular cross sections which therefore needed careful alignment with the centre of the charge. Dewey [28] used the deformation of solder cantilevers to compare the energy yields of TNT and ANFO explosions. Some researchers have added spheres and cylinders to the tops of cantilevers in order to make them more sensitive to the drag forces, but such additions add to the complexity of the analysis of the cantilever's motion, and when rectangular or cylindrical appendages are used, careful alignment of the cantilever with the centre of the charge is required. Simple cylindrical cantilevers are the easiest to deploy and analyse. Because of their cylindrical symmetry they do not need to be accurately aligned with the centre of the charge, and in fact, the direction of bending provides an accurate measure of the direction of the charge centre, so that the centre of an explosion can be identified from the directions of bending of two cantilevers at different azimuthal positions. van Netten and Dewey [6] provides the most detailed study of cantilevers exposed to blast waves; how they may be used to determine some properties of blast waves, and measure the energy yield of an explosion as it relates to TNT and ANFO.

Because of its small cross-section, a cylindrical cantilever is essentially insensitive to the hydrostatic pressure and responds only to the dynamic or drag forces. Two types of material have been used to make cantilever gauges: brittle, and ductile. Brittle cantilevers fail almost immediately after the passage of the primary shock, and can therefore be used to assess the peak drag force immediately behind the shock. Ductile cantilevers respond more slowly and are subjected to the total duration of the drag force so that their final bend angle can be related to the drag impulse.

Brittle cantilever gauges have been made from glass rods for measurements relatively close to the explosion, and from pencil leads for use at greater distances. Both of these materials are readily available and are consistent in their properties, especially the pencil leads. Brittle cantilevers are deployed at a location in an array of different lengths. The longer cantilevers are subjected to greater loading, thus placing greater stress at the base of the cantilever where it is held in its mount. As a result, for an ideal measurement, the longer cantilevers will fail while the short ones will remain intact. The length of the shortest cantilever to fail is used to assess the peak drag force at that location.

Ductile cantilevers have been made from steel, aluminium and solder. All of these materials are easily available in cylindrical form with a range of diameters, and are consistent in their properties if the appropriate metal type is chosen. Short, e.g. 20 cm long, 2.5 cm diameter steel rods have been used at very high pressures close to the rim of the crater of a large surface burst explosion where they were buried by the ejecta from the crater, and were strong enough not to be affected by the falling

Fig. 10 A 2.5 cm diameter aluminium rod cantilever after exposure to a blast wave, showing that the rod bends only at the end where it was held in concrete



debris. Aluminium rods of various lengths and diameters have been used to study blast waves at intermediate distances, see Fig. 10, and solder has been used in regions of low loading pressure. The rod shown in Fig. 10 was photographed against a rectangular grid orientated horizontally with a spirit level so that the degree of bending could be measured from the photograph. The length, diameter and material of the cantilever were chosen so that the predicted blast wave properties at the location of the gauge would produce a bend angle of approximately 45° .

Examples of the use of such cantilever gauges are given by van Netten and Dewey [29, 30]. Methods of choosing the appropriate size and material for a cantilever gauge, based on the estimated properties of the blast wave to which it is to be exposed are given by van Netten and Dewey [6].

Cantilever gauges are sensitive to the dynamic or drag forces within a blast wave which change significantly in the boundary layer over the ground, from effectively zero at the ground surface to the free-field levels above the boundary layer. At high and intermediate loading levels, where the boundary layer is relatively thin, cantilever gauges can be mounted in the ground, but at intermediate levels it is preferable to use relatively long cantilevers so as to minimise the boundary layer effect. At lower loading levels cantilever gauges should be mounted on stands at least 30 cm above the ground, which seems to be a typical boundary level height in blast waves.

At high and intermediate pressure levels cantilevers can be installed in the ground embedded in concrete. At lower pressure levels where cantilevers need to be supported on stands to avoid the boundary layer, they should be mounted in sharp edged baffles with a smooth transition from the bevelled edge to the level surface where the cantilevers are mounted. The cylindrical cantilevers are inserted in holes drilled in the baffle and may need a small amount of glue to ensure that they are not loose.

Horizontal cantilevers are an excellent way of determining the height of the boundary layer in a blast wave. For this purpose they are mounted in a vertical baffle with sharp leading and trailing edges, which needs to be carefully aligned with the centre of the explosion. The cantilevers are mounted horizontally in the baffle in a vertical array with a spacing of a few centimeters. Both sides of the

baffle can be used. After the passage of the blast wave the decrease in bending of the cantilevers close to the ground relative to those at higher levels clearly indicates the extent of the boundary layer. This is illustrated in van Netten and Dewey [30].

3.10.2 Estimating Blast Properties from Damage and Injury

In the case of accidental explosions normally there will be no direct measurements of blast wave properties, but gross measures of properties, such as the TNT equivalence of an explosion, can often be estimated from the distances at which certain damage or injury has occurred. Such assessment becomes more difficult if there have been multiple explosions. Most blast damage is caused by the drag or dynamic pressure loading rather than the hydrostatic pressure, but because of the difficulty of measuring dynamic pressure most blast damage and injury criteria are expressed in terms of the peak hydrostatic pressure and its impulse over the positive phase. Except for cases of rapidly responding structures such as eardrums or thin glass windows, blast damage depends on both the peak loading and on the loading duration. This is related to the amount of energy released in an explosion, and the rate at which the energy was released. A massive structure may sustain little damage from a small explosive device, even though it is placed very close to the structure where the peak loading pressure may be many atmospheres, but the loading duration is only a few milliseconds. That same structure may be totally destroyed by the blast from a nuclear weapon when the peak loading pressure is less than 1 atm, but the duration of the loading is several seconds.

Because any specific level of damage or injury occurs at a high pressure from a small explosion and at a lower pressure but longer duration from a larger explosion, the relationship between the peak pressure and the impulse for that damage level has the approximate form of a rectangular hyperbola. An idealised damage criterion curve is shown in Fig. 11. The curve approximates a rectangular hyperbola in the peak-hydrostatic-pressure—hydrostatic-pressure-impulse plane. If at a location in a blast wave the point represented by the hydrostatic peak pressure and impulse lies above the criterion curve, damage/injury is likely to occur. If it lies below the curve, damage/injury is unlikely to occur. The pressure asymptote indicates the minimum pressure, which if continuously applied, would produce the damage or injury. The impulse asymptote indicates the minimum duration below which damage or injury would not occur, no matter how large the pressure.

Damage criterion curves can only be used to give a rough estimate of the likelihood of damage because of the limited amount of information available for a specific type of damage or injury over a wide range of charge sizes. Many of the existing damage and injury criteria were developed for nuclear explosions, or, in the case of intermediate size explosions, from studies of damage produced during the Blitz in the United Kingdom during WWII. Much less information is available for smaller explosions, which are the main concern at the present time. There seems to be no published compendium of blast wave damage and injury criteria, but information can be found by searching the Internet. The application of damage and

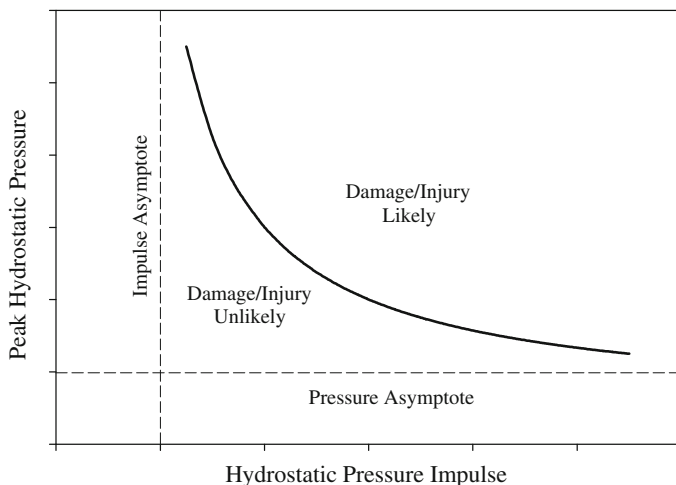


Fig. 11 An idealized damage/injury criterion curve

injury criteria curves is discussed in some detail in Dewey and van Netten [31], and specifically for cantilever bending in van Netten and Dewey [6]. In particular, the latter reference describes how a certain level of damage can be used to estimate the TNT mass equivalence of an explosion.

3.11 Measurement Methods Using Numerical Simulation

For several decades numerical simulation has become a major tool in the estimation of the physical properties of blast waves. The calculation of the physical properties within an established blast wave is relatively straightforward, but a calculation of the detonation process requires an accurate knowledge of the complex chemical and physical processes in such an event. Few hydro-codes have this ability. The code that seems to have been most successful in solving this problem is SHAMRC (see www.ara.com). Numerical simulation techniques need to be carefully validated by comparison with physical measurements of the blast wave properties. It must be stressed that comparison with measurements of the hydrostatic pressure only has proved to be unreliable, and validation comparisons must be made with measurements of such properties as density, particle velocity and particle displacement.

A powerful measurement technique is a combination of direct physical measurement with a numerical simulation. In this technique the starting processes of the simulation are iteratively adjusted until the calculated physical properties match a series of measured properties as accurately as possible. An example of such a process is the piston path method (PPM). Taylor [32] showed that a blast wave from a centred source could be generated by a spherical piston with an appropriate radius-time trajectory: the piston path. This trajectory can be determined

experimentally by high-speed photography of smoke tracers initiated close to an explosive charge immediately before its detonation. Examples of the use of this technique are given by Dewey and McMillin [21, 22]. In these examples, the results from the piston path calculations were compared with many hundreds of measurements of hydrostatic pressure, dynamic pressure and density made using electronic transducers, and the excellent agreement validated the technique.

More recently, it has been shown that the piston-path technique can be used to determine all the physical properties of a centred blast wave in the radius-time plane using only the measured radius-time trajectory of the primary shock (Dewey and Dewey [19]). In this method an arbitrary piston-path is used in a hydro-code to generate a blast wave, the primary-shock trajectory of which can be compared with the measured trajectory. The piston path was defined by a series of nodes. The nodes were iteratively adjusted until a piston path was obtained that generated a blast wave whose primary-shock trajectory exactly matched the measured values.

A similar method has been used in which the numerical simulation is driven by a sphere of high-temperature high-pressure gas. The initial pressure and temperature can be set to approximate the expected energy yield of the source. The energy yield and the rate of energy release can be adjusted until a blast wave is obtained that matches as closely as possible a set of measured values.

4 Blast Wave Scaling Laws

The physical properties of a spherically expanding blast wave, expressed either as wave profiles at specific times or as time histories at specific distances, are not self-similar. This means that a profile or time history measured at one time or distance cannot be scaled to a profile or time history at another time or distance. However, the physical properties are subject to precise scaling laws relating to the amount of energy released at the source and the properties of the ambient gas into which the shockwave is expanding.

Hopkinson [33] and Cranz [34] originally defined the scaling laws for blast waves. They showed that the distance from the centre of an explosive charge of a physical property's peak value immediately behind the primary shock, and the positive duration of that property are proportional to the linear dimension of the spherical charge. The linear dimension of the charge is also proportional to the cube root of the charge mass. If a property value or positive duration occurs at a distance R_1 from a charge of mass W_1 and at a distance R_2 from a charge of the same material with a mass W_2 then

$$\frac{R_2}{R_1} = \left(\frac{W_2}{W_1} \right)^{1/3} \quad (34)$$

Normally, W_1 is set at a unit charge mass of 1 kg or 1 kt. The charge mass W can be replaced by the calculated energy content of the source, E , but this may be less

reliable than using the charge mass because it is not known what percentage of the energy is released as thermal or other forms of radiation, or, if the explosion is close to the ground, how much of the energy is used in making a crater, or is dissipated as seismic waves.

Sachs [35] augmented the cube root scaling law for mass to account for differences in the ambient atmospheric pressure, P_0 , and temperature, T_0 , of the gas into which the shockwave is moving. Sachs stated that: (a) the magnitudes of hydrostatic pressure, density and absolute temperature scale in proportion to their values in the ambient gas; (b) distances and durations will scale in inverse proportion to the cube root of the ambient pressure, and (c) durations and times of arrival will be proportional to the sound speed in the ambient gas, and thus to the square root of the ambient absolute temperature. Equation (34) therefore becomes

$$\frac{R_2}{R_1} = \left(\frac{W_2}{W_1} \right)^{1/3} \left(\frac{P_{01}}{P_{02}} \right)^{1/3} \quad (35)$$

where P_{01} and P_{02} are the ambient pressures for the two explosions. Times of arrival of the primary shock and times of duration within the blast wave scale as

$$\frac{t_2}{t_1} = \left(\frac{W_2}{W_1} \right)^{1/3} \left(\frac{P_{01}}{P_{02}} \right)^{1/3} \left(\frac{T_{01}}{T_{02}} \right)^{1/2} \quad (36)$$

where T_{01} and T_{02} are the ambient absolute temperatures in degrees Kelvin, viz. $T^\circ \text{ K} = T^\circ \text{ C} + 273.16$. To scale measured values of distance and time to those expected for a unit charge in an ambient atmosphere at Normal Temperature and Pressure (NTP), W_1 is set at 1 kg, $P_{01} = 101.325 \text{ kPa}$ and $T_{01} = 288.16 \text{ K}$. Measurements scaled in this way provide a comparison with the blast waves from other explosions of different masses of the same explosive in different ambient atmospheric conditions. The validity of these scaling procedures has been demonstrated by Dewey and Sperrazza [36] and Dewey [5].

5 Summary and Discussion

The electronic pressure transducer remains the principal device for monitoring the physical properties of blast waves, but its limitations, described in Sects. 2.1.1 and 3.2, must be remembered. In particular, the hydrostatic pressure measured by a flush mounted gauge does not detect the passage of a contact surface between two gases which may have very different densities and temperatures. Neither does it detect variations of flow velocity, nor therefore the dynamic pressure, that occur in the boundary layer as a blast wave passes over the ground or a structure. Pressure transducers flush mounted in the surface of a structure are required to measure the loading pressures on the structure exposed to a blast wave.

Passive gauges such as cantilevers can be valuable tools to monitor blast waves, even though they do not provide precise measures of the physical properties. Some of their principal advantages are that they are cheap; can be left in place for long periods without attention; provide an accurate reading of the direction towards the centre of the blast, and can be quickly and easily interpreted. Therefore, they are particularly useful for deployment in an area in which there is the possibility of an accidental or unscheduled explosion. They can also be used to rapidly compare the blast waves from a sequence of explosions carried out in quick succession.

High-speed photography remains a powerful tool to monitor blast waves both qualitatively and quantitatively. Its unique advantage is that it provides information about large regions of the blast wave and not at just a few specific locations. Refractive image analysis is undoubtedly the most accurate method for measurement of the position and velocity of the primary shock front. In this regard, it is more accurate for measurements of the peak values immediately behind the primary shock than electronic transducers, the signals from which do not provide an accurate measure because of overshoot, ringing or damping.

All of the physical properties of a centred blast wave can be determined from high-speed photography of the time-resolved displacement of flow tracers established shortly before the arrival of the primary shock, and is one of the few techniques that provides a complete mapping of all the physical properties in the radius-time plane. Background oriented schlieren (BOS) shows promise in being able to map the density field in an axisymmetric or centred blast wave but the technique has not been fully validated, and the resolution of the density field close to the primary shock has yet to be demonstrated. Also, this technique maps only the density field and does not provide information about other physical properties such as hydrostatic pressure and particle velocity.

Numerical simulation of blast waves and their interaction with structures, using suitable hydro-codes, is a powerful technique that maps all the physical properties but must be validated using direct measurements, ideally of other physical properties in addition to pressure. This is particularly important when using numerical simulation to study phenomena such as blast mitigation. Most numerical simulations assume that there is no energy loss in a blast-structure interaction. The energy of a blast wave has two components, one associated with the hydrostatic pressure and the other with the dynamic pressure. If, therefore, the hydrostatic pressure is reduced there must be a corresponding increase of the dynamic pressure, which is usually the more damaging of the two components. It is important that the dynamic pressure be calculated using the form of Eq. (1) so that the dynamic pressure is a vector rather than a scalar quantity. In this way it can be determined if a reduction in hydrostatic pressure has resulted in an increase of any component of the dynamic pressure. Only if the hydrostatic pressure and the components of the dynamic pressure have been reduced can mitigation of the blast be said to have occurred.

The most powerful technique of measuring all the physical properties of a centred or axisymmetric blast wave is undoubtedly one that uses a combination of direct measurement and numerical simulation, such as particle trajectory analysis (PTA) described in Sect. 3.9.2. The simplest way of doing this may be that

described by Dewey and Dewey [19] in which the numerical simulation is iteratively adjusted until one set of calculated properties exactly matches the corresponding set of measurements. The easiest and cheapest set of such measurements is the times of arrival of the primary shock, which can be obtained from an array of simple switches, the signals from which can be transmitted through a single cable to a timed recording channel.

It is important that all measurement devices, particularly pressure transducers, be calibrated regularly, ideally before and after each use. Most pressure transducers will be accompanied by a manufacturer's calibration curve relating the applied over- or under-pressure to the output signal over the range of pressures to which the transducer is to be submitted. Ideally this curve will be linear, but that should not be assumed. Wherever possible, the calibration should be carried out using the transmission cabling, the amplifiers and the recording channel that will be used on the test. The calibrations over the range of expected over-pressures are best done in a shock-tube type device in which the shock velocity can be measured by a pair of time-of-arrival detectors as it passes the transducer. The ambient pressure and temperature must also be measured so that the shock Mach number can be calculated and used in the Rankin-Hugoniot relationship (5) to determine the pressure immediately behind the shock. Calibration in the under-pressure range can be done using a device similar to the driver section of a shock tube in which an applied pressure is rapidly released by the rupture of a diaphragm or fast acting valve.

In order that the measured physical properties of a blast wave can be compared with those from other explosions, the properties should be expressed in terms of the ambient pressure, temperature and density at the time of the explosion and scaled to those from a unit charge in an atmosphere at NTP, as described in Sect. 4. To do this, the ambient values of pressure, temperature and wind velocity should be measured as close to the explosive source and time of detonation as possible. The ambient temperature is usually measured at a height of about 2 m to avoid the large temperature gradients that may occur close to the ground, and at higher altitudes for large charges. Scaling of blast waves also requires knowledge of the charge mass, and this should be measured as accurately as possible. It may be unreliable to use the manufacturer's value for charge mass which is often related to the volume of the mould in which the charge was made, rather than a direct measurement of mass. The charge mass provided by the manufacturer should be treated with particular suspicion if it exactly matches the specified or nominal mass. The charge mass used in scaling must include the mass of any booster charge.

The locations of all measurement devices, cameras, fiducial markers used to scale photographic measurements, and the positions of structures being exposed to the blast must be surveyed accurately relative to the centre of the explosion, and to each other. Experience has shown that survey errors are not uncommon, and for tests on which there is a large amount of instrumentation it may be appropriate to have dual, independent surveys so that such errors can be identified.

References

1. Brouillette, M.: The Richtmyer-Meshkov instability. *Annu. Rev. Fluid Mech.* **34**, 445–468 (2002)
2. Needham, C.E.: *Blast Waves*. Springer, Heidelberg (2010)
3. Dewey, J.M.: Expanding spherical shocks (blast waves). In: Ben-Dor G, Igra O, Elperin T (eds.) *Handbook of Shock Waves*, Vol. 2, pp. 441–481. Academic Press, San Diego (2001)
4. Dewey, J.M., McMillin, D.J., van Netten, A.A., Ethridge, N., Keefer, J., Needham, C.E.: A study of the boundary layer in a large scale blast wave over a natural surface. In: *Proceedings of 14th International Symposium on Military Aspects Blast and Shock (MABS14)*, Las Cruces, NM, USA, Defense Threat Reduction Agency, pp. 1–28 (1995)
5. Dewey, J.M.: The air velocity in blast waves from t.n.t. explosions. *Proc. Roy. Soc. A* **279**, 366–385 (1964)
6. van Netten, A.A., Dewey, J.M.: A study of the blast wave loading on cantilevers. *Shock Waves* **7**, 175–190 (1997)
7. Reisler, R.E., Keefer, J.H., Ethridge, N.H.: Air blast instrumentation, 1943-1993, measurement techniques and instrumentation: vol. 1, the nuclear era, 1945-1963; Vol. 2 the high explosive era, 1959-1963, and Vol. 3 air blast structural target and gage calibration. In: *MABS Monograph*, Defence Nuclear Agency (now Defence Threat Reduction Agency), Alexandria, VA, USA
8. Dewey, J.M.: Blast wave measurement techniques: photo-optical methods. In: *Proceedings of 13th International Symposium on Military Applications of Blast Simulation (MABS 13)*, pp. 1–15, Division Defence Technology, Royal Institution of Engineers in the Netherlands (Klvi), The Hague, The Netherlands (1993)
9. Dewey, J.M.: Shock waves from explosions. In: Ray SF (eds.) *High-Speed Photography and Photonics*. Focal Press, Oxford (1997)
10. Dewey, J.M.: Explosive flows: shock tubes and blast waves. In: Yang W-J (eds.) *Handbook of Flow Visualization*, 2nd Edn. Hemisphere, New York (1997)
11. Dewey, J.M.: The Rankine-Hugoniot equations: their extensions and inversions related to blast waves. In: *Proceedings of 19th International Symposium on Military Aspects Blast and Shock (MABS19)*, Can. Def. Res. Suffield, Alberta, Canada, P008 (2006)
12. Dewey, J.M.: The TNT equivalence of an optimum propane-oxygen mixture. *J. Phys. D Appl. Phys.* **38**, 4245–4251 (2005)
13. Dewey, J.M.: The properties of a blast wave obtained from an analysis of the particle trajectories. *Proc. Roy. Soc. Lond. A* **324**, 275–299 (1971)
14. Kleine, H., Dewey, J.M., Ohashi, K., Mizukaki, T., Takayama, K.: Studies of the TNT equivalence of silver azide charges. *Shock Waves* **13**, 123–138 (2003)
15. Dewey, J.M., Anson, W.A.: A blast wave density gauge using beta-radiation. *J. Sci. Instr.* **40**, 568–572 (1963)
16. Ritzel, D.V.: Blast-wave density measurements. In: Bershader, D., Hanson, R. (eds.) *Proceedings of 15th International Symposium on Shock Waves and Shock Tubes*, Stanford Univ., Berkley, California, 578–585 (1985)
17. Slater, J.E., Boechler, D.E., Edgar, R.C.: DRES measurement of free-field airblast. In: *Minor Uncle Symposium Report*, Defense Nuclear Agency, POR 7453-4, Vol. 4, 2, pp. 1–98 (1995)
18. Liepmann, H.W., Roshko, A.: *Elements of Gasdynamics*. Wiley, New York (1957)
19. Dewey, J.M., Dewey, M.C.: The physical properties of the blast wave produced by a stoichiometric propane/oxygen explosion. *Shock Waves*, **24**, 593–601 (2014)
20. Harvey, R.B., Lutz, H.B.: Photo-optical studies of nuclear airblast, operations BUFFALO (1956) and ANTLER (1957): measurements of elapsed time, Vol. 4, Pt 2, TTCP Panel TLG3/0004, Atomic Weapons Establishment, Ministry of Defence, Aldermaston, UK (1988)
21. Dewey, J.M., McMillin, D.J.: Smoke puff photo-diagnostics. In: *MISERS GOLD Symposium Report*, Defence Nuclear Agency, Alexandria, VA, POR 7352-2, Vol. II (1991)

22. Dewey, J.M., McMillin, D.J.: Smoke trail photo-diagnostics. In: MINOR UNCLE Symposium Report, Event Diagnostics and Calculations, Vol. 2, pp. 2-1–2-48, Defence Nuclear Agency, Alexandria, VA, POR 7453-2 (1995)
23. Venkatakrishnan, L., Meier, G.E.A.: Density measurements using the background oriented Schlieren technique. *Expt. Fluids* **37**, 237–247 (2004)
24. Ramanah, D., Raghunath, S., Mee, D.J., Rösigen, T., Jacobs, P.A.: Background oriented schlieren for flow visualisation in hypersonic impulse facilities. *Shock Waves* **17**, 65–70 (2007)
25. Penny, Lord: The nuclear explosive yields at Hiroshima and Nagasaki. *Roy. Soc. Phil. Trans.* **266**, 357–424 (1969)
26. Ewing, W.O., Hannah, J.W.: A Cantilever for Measuring Air Blast, Ballistic Research Laboratories. Tech. Note 1139 (1957)
27. Baker, W.E., Ewing, W.O., Hannah, J.W.: Laws for large elastic response and permanent deformation of model structures subjected to blast loading. Ballistic Research Laboratories, Rept. 1060 (1958)
28. Dewey, J.M.: Surface burst of a 100 ton TNT hemispherical charge: Wire drag gauge measurements, Suffield Experimental Station, Technical Note 80 (1962)
29. Van Netten, A.A., Dewey, J.M.: Cantilever gauges. In: Proceedings of DISTANT IMAGE Symposium, Defense Nuclear Agency, POR7379-5, p. 5 (1992)
30. Van Netten, A.A., Dewey, J.M.: Horizontal cantilever gauges and cantilever gauges. In: Proceedings of MINOR UNCLE Symposium, Defense Nuclear Agency, POR7453-5, p. 5 (1995)
31. Dewey, J.M., van Netten, A.A.: Calculating blast effects distances in urban environments. In: Proceedings of 17th International Symposium on Military Aspects Blast and Shock (MABS17), Blast and Shock Effects, US Department of Defense, p. 8 (2002)
32. Taylor, Sir G.I.: The air waves surrounding an expanding sphere. *Proc. Roy. Soc. Lond. A* **186**, 273–292 (1946)
33. Hopkinson, B.: British Ordnance Board Minutes, 13565 (1915)
34. Cranz, C.: *Lehrbuch der Ballistik*. Springer, Berlin (1926)
35. Sachs, R.G.: The dependence of blast on ambient pressure and temperature. BRL Report 466, Aberdeen Proving Ground, Maryland, USA (1944)
36. Dewey, J.M., Sperrazza, J.: The effect of atmospheric pressure and temperature on air shock, BRL Report 271, Aberdeen Proving Ground, Maryland, USA (1950)

Author Biography



John Dewey received his B.Sc. and Ph.D. in Physics from the University of London. He has studied the physical properties of blast waves since 1956, first at the Defence Research Establishment Suffield, where he was Head of the Aerophysics Section, and then at the Department of Physics and Astronomy at the University of Victoria, Canada, where he established and ran the Shock Studies Laboratory for over 30 years. He specialized in the use of high-speed photographic techniques for the study of shock and blast waves in shock tubes and on many hundreds of field experiments involving explosive charges ranging from 1 mg to 5 kt. He has published more than 135 journal papers, articles and chapters.

Experimental Methods of Shock Wave Research

Igra, O.; Seiler, F. (Eds.)

2016, X, 478 p. 443 illus., 232 illus. in color., Hardcover

ISBN: 978-3-319-23744-2